Supplementary Information

for

Coordination and oxidation properties of ZBTB20: $CX_2CX_{12}HX_3H$-type zinc fingers

Hyunyong Kim,[a]‡ Yunha Hwang,[a]‡ Hyunwoo Jung,[b] Jin Sung Cheong,[c] Jiyeon Han,*[b] and Seung Jae Lee*[a,d]

[1]Department of Chemistry, Jeonbuk National University, 54896 Jeonju, Republic of Korea.

[2]Department of Applied Chemistry, University of Seoul, Seoul 02504, Republic of Korea

[3]Department of Neurosurgery, Wonkwang University Hospital, Iksan 54538, Republic of Korea.

[4]Research Institute for the Molecular Biology and Genetics, Jeonbuk National University, 54896 Jeonju, Republic of Korea.

‡These authors contributed equally to this work.

*To whom correspondence should be addressed: slee026@jbnu.ac.kr and jiyeonhan@uos.ac.kr

Table of Contents

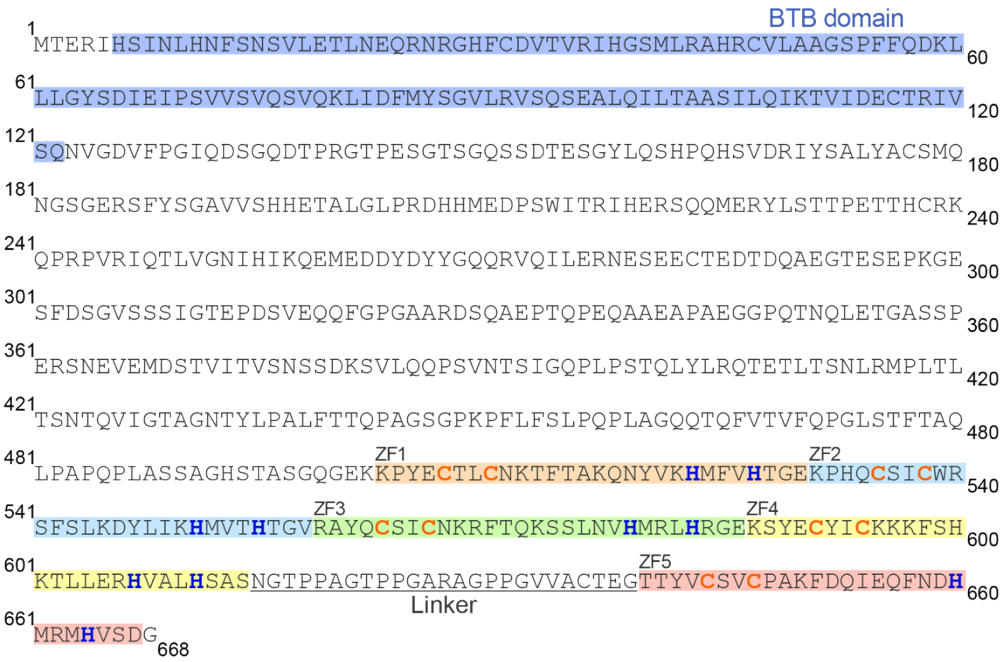

Figure S1. Amino acid sequence of ZBTB20 from *Homo sapiens* (NCBI: AAH29041.1).[1] The BTB domain is highlighted in dark blue. Each zinc finger domain (ZF1–5) is highlighted in a distinct color: ZF1 in orange, ZF2 in light blue, ZF3 in light green, ZF4 in yellow, and ZF5 in salmon pink. Zn^{2+}–coordinating cysteine residues are shown in orange, and histidine residues are indicated in blue. The linker sequence connecting ZF4 and ZF5 is underlined in blue.

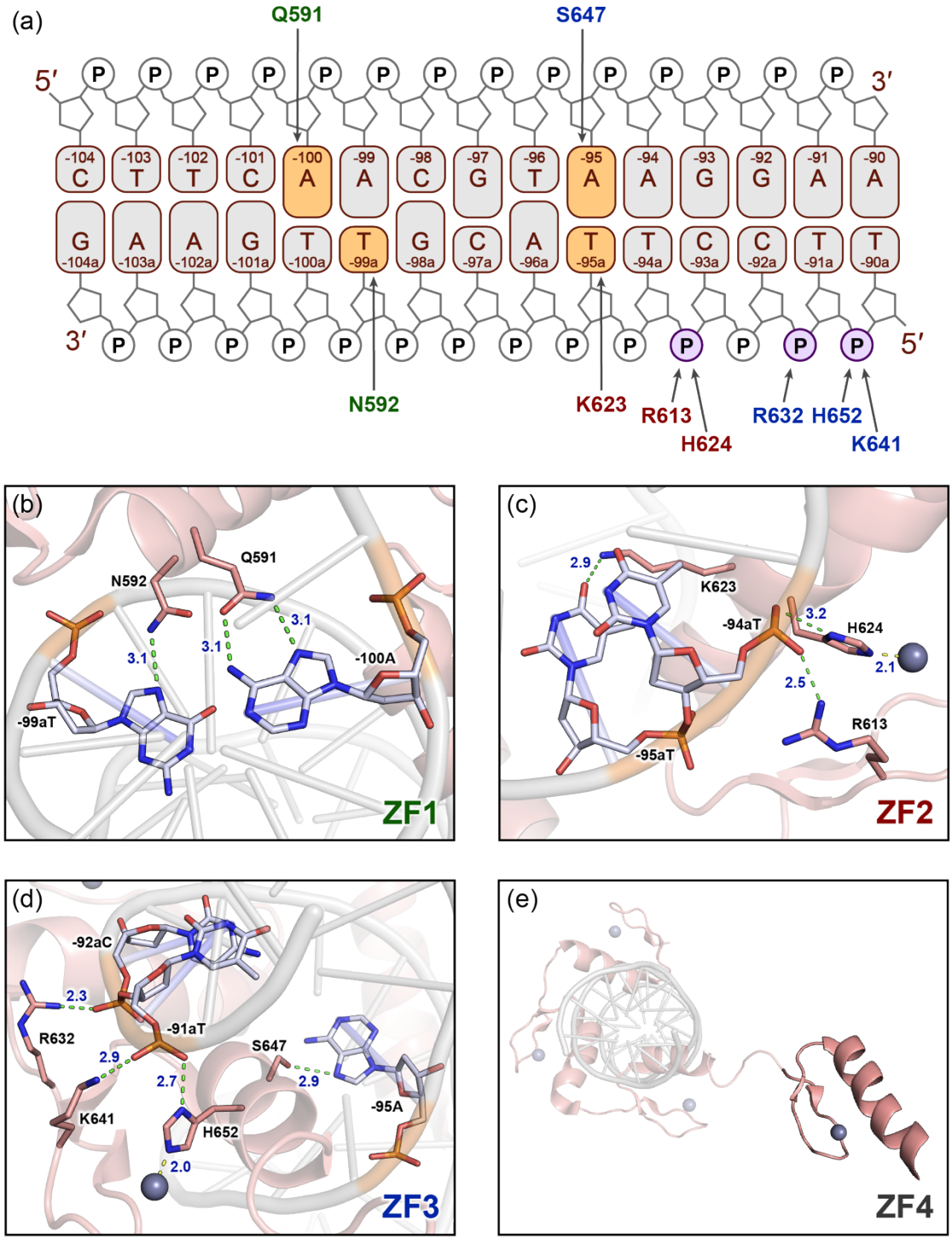

Figure S2. Structural basis of the ZBTB20(ZF1–4)-mediated recognition of the *afp* promoter.[2] (a) Ladder diagram illustrating the DNA sequence within the mouse *afp* promoter and the specific nucleotides

contacted by each ZF domain of mouse ZBTB20. The upper and lower strands represent the sense and antisense strands, respectively, and residues engaging in base-specific or phosphate-backbone interactions are indicated above or below the corresponding nucleotide positions. (b–e) Structural depiction of the contacts formed between the mouse *afp* promoter and (b) ZF1, (c) ZF2, (d) ZF3, (e) ZF4. The gray sphere represents the Zn^{2+} ion. Hydrogen bonds are shown as green dashed lines, and coordination bonds to Zn^{2+} are indicated by yellow dashed lines.

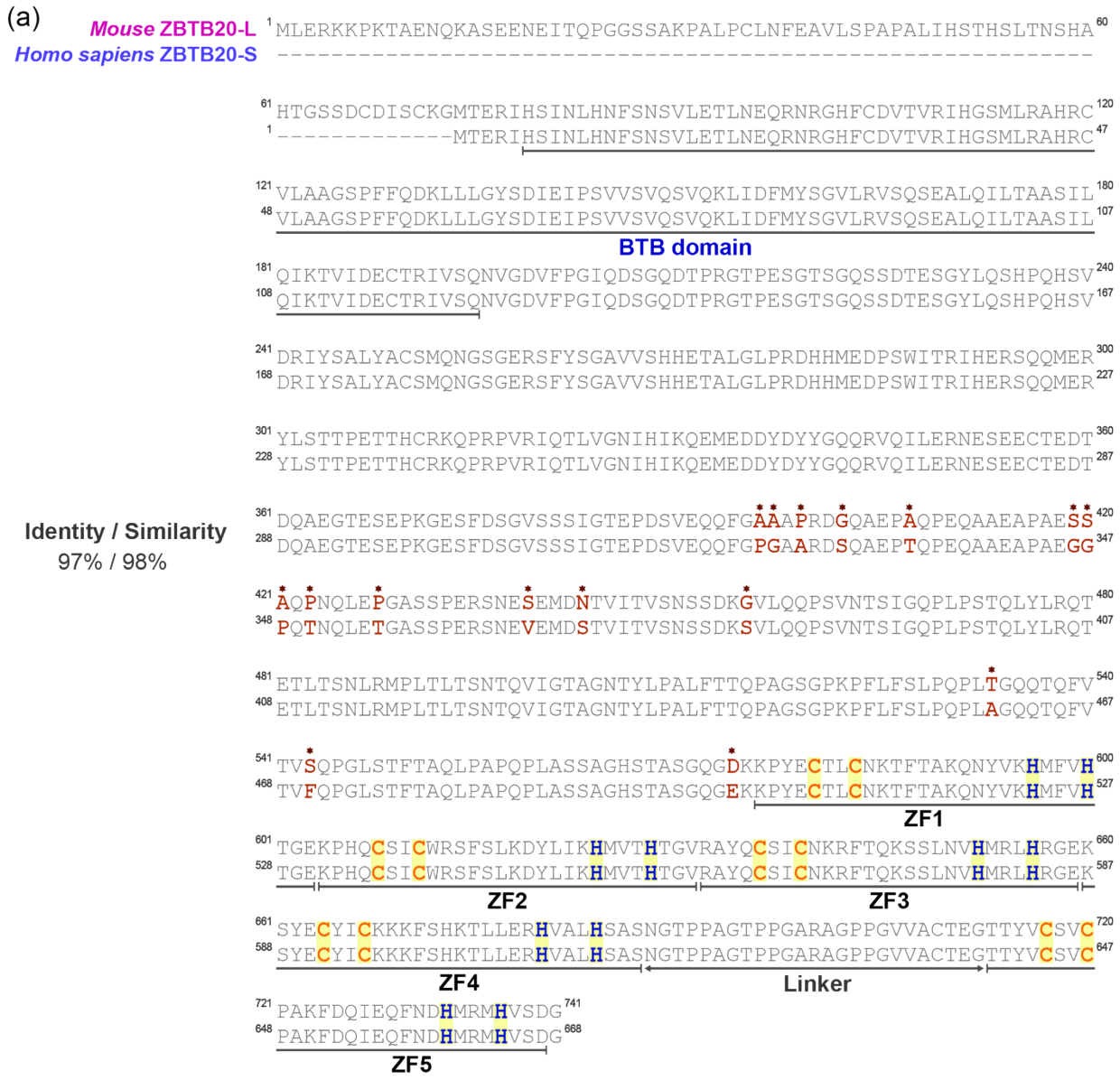

Figure S3. Sequence alignment of mouse ZBTB20 and *Homo sapiens* ZBTB20.[2] Mismatched residues are shown in red bold with a star, and cysteine and histidine in each ZF domain are highlighted with colored boxes.

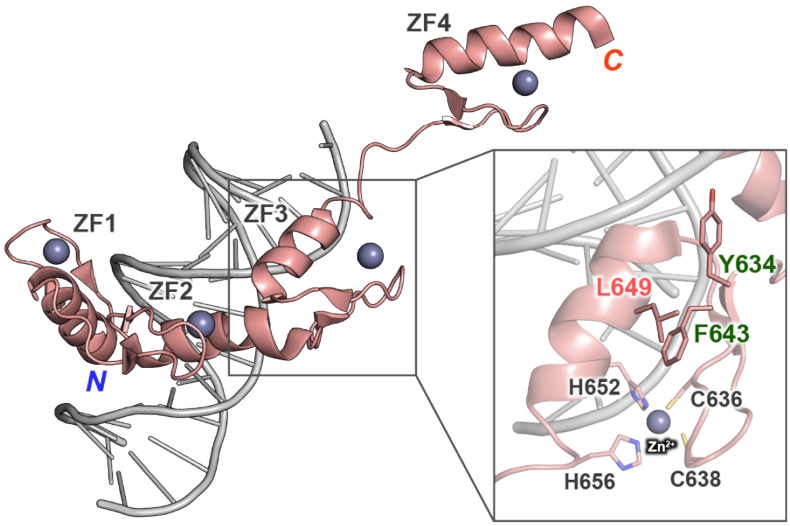

Figure S4. Crystal structure of mouse ZBTB20(ZF1–4) bound to the mouse *afp* promoter (PDB: 9JZT).[2] Zinc ions are depicted as gray spheres. The inset highlights residues in ZF3—Tyr634, Phe643, and Leu649—that form a hydrophobic core positioned adjacent to the Zn^{2+}–coordinating cysteine and histidine residues, contributing to local structural stability and maintaining the DNA-binding geometry.[3]

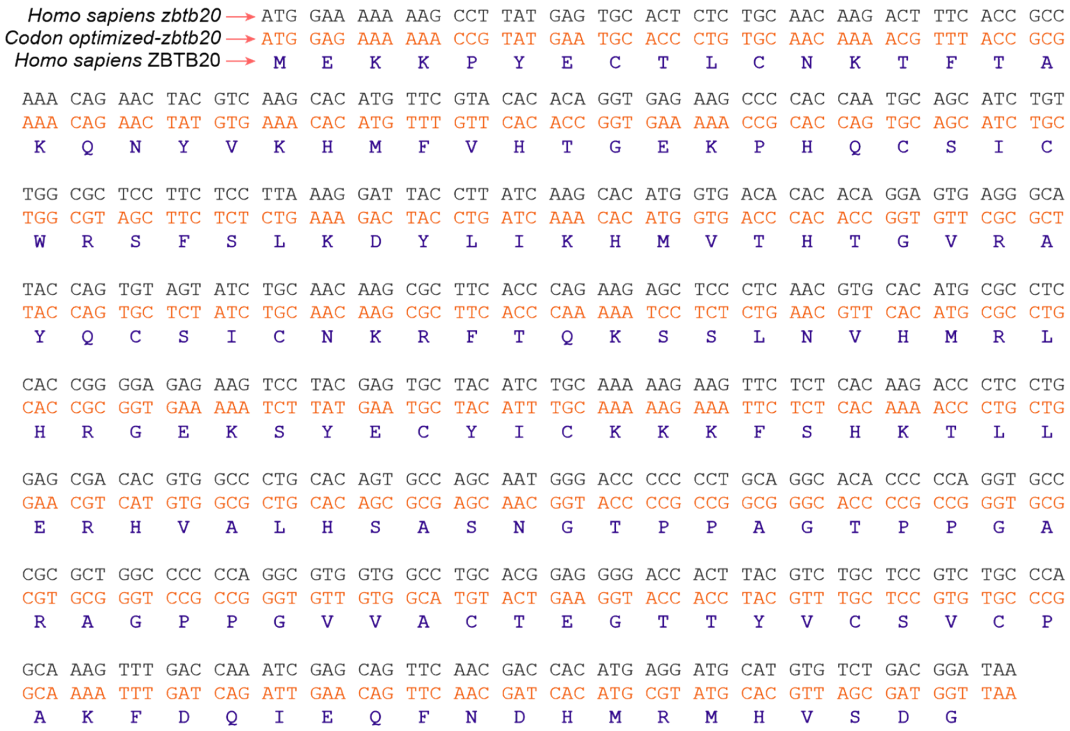

64

65 **Figure S5.** Codon-optimized DNA sequence of ZBTB20(ZF1–5) from *Homo sapiens*. Comparison of the
66 *zbtb20* DNA sequence (NCBI: BC029041.1) with its codon-optimized version for *Escherichia coli*
67 expression. The original sequence is shown in black, and codon-optimized nucleotides are indicated in
68 orange. The corresponding amino acid sequence of ZBTB20(ZF1–5) is shown in bold purple below each
69 codon.

70

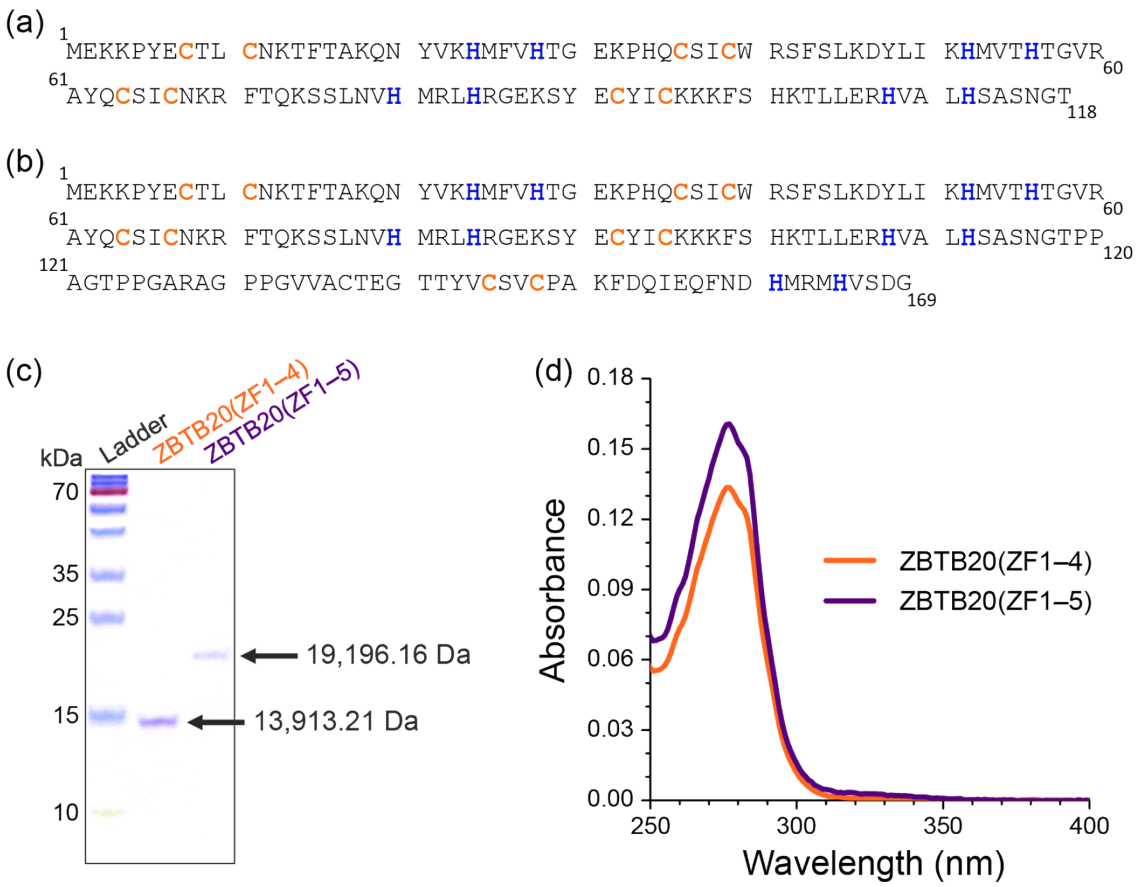

Figure S6. Sequence and characterization of purified ZBTB20(ZFs). (a–b) Amino acid sequences of (a) ZBTB20(ZF1–4) and (b) ZBTB20(ZF1–5). Zn^{2+}–coordinating cysteine residues are shown in orange and histidine residues in blue. (c–d) SDS-PAGE analysis and UV–Visible spectra of purified (c) ZBTB20(ZF1–4) and (d) ZBTB20(ZF1–5). For SDS-PAGE, ZBTB20(ZF1–4) and ZBTB20(ZF1–5) were diluted to 15 µM and 10 µM, respectively. UV–Vis spectroscopy was performed using 8 µM ZBTB20(ZF1–4) and 9 µM ZBTB20(ZF1–5).

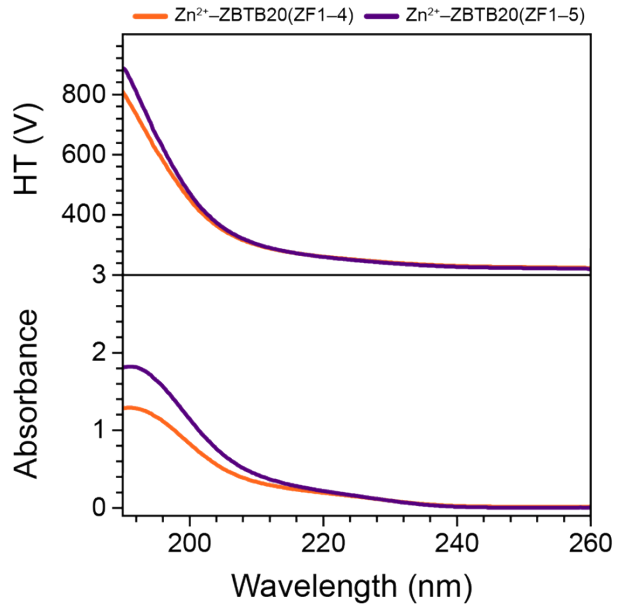

Figure S7. HT voltage and absorbance recorded during CD measurements of ZBTB20(ZFs). Changes in HT voltage, and absorbance of Zn^{2+}–ZBTB20(ZF1–4) and Zn^{2+}–ZBTB20(ZF1–5). The HT and absorbance were monitored in parallel during CD measurements. All measurements were performed at a protein concentration of 20 μM in 20 mM HEPES (pH 7.4) containing 150 mM NaF. CD spectra were collected using a 0.5-mm quartz cuvette with a 2-nm bandwidth and a scanning speed of 50 $nm \cdot min^{-1}$.

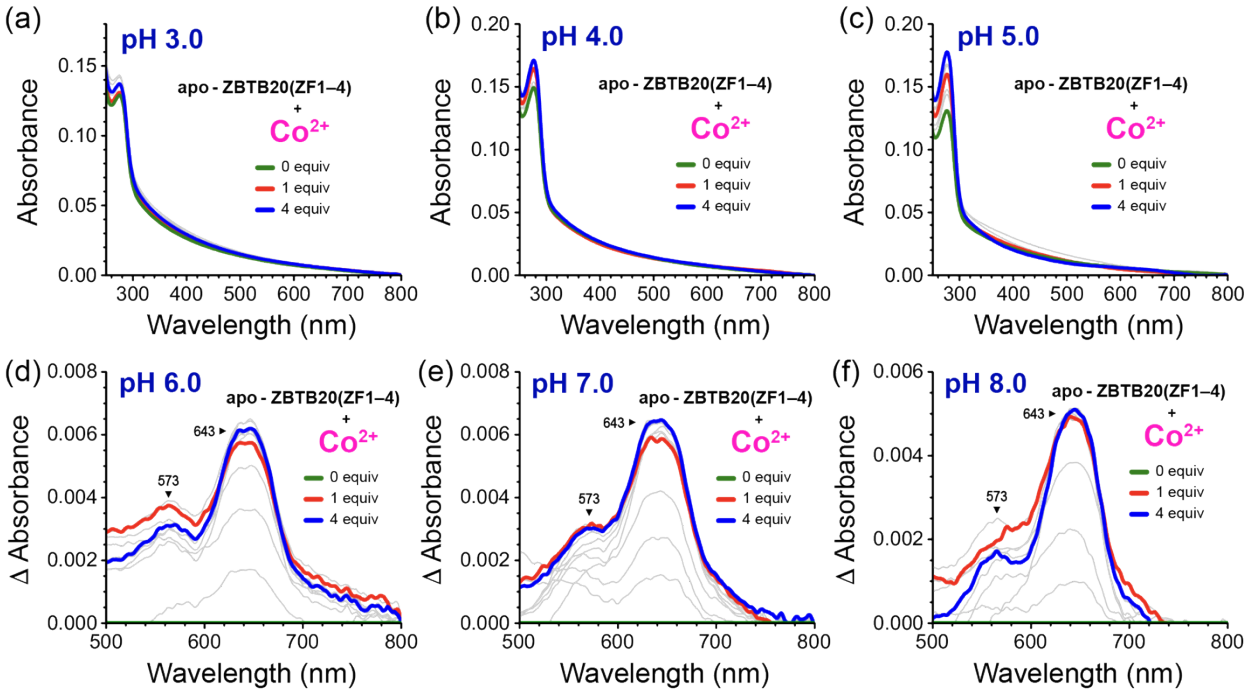

84

85

86 **Figure S8.** pH-dependent oxidation of apo-ZBTB20(ZF1–4). d–d transition bands were measured using a
87 UV–Visible spectrophotometer, and the % metal bound under each condition was calculated from the
88 absorbance maxima at 643 nm.[4] Δ Absorbance represents the changes in absorbance relative to apo-
89 ZBTB20(ZF1–4) upon Co^{2+} titration. Experiments were conducted at (a–c) pH 3.0, 4.0 and 5.0 (100 mM
90 sodium acetate), (d) pH 6.0 (100 mM MES monohydrate), (e) pH 7.0 (100 mM MOPS), and (f) pH 8.0 (100
91 mM Tris), with all buffers containing 150 mM NaCl and 1 mM TCEP. Each experiment was performed
92 inside an N_2(g)-filled glovebox.

93

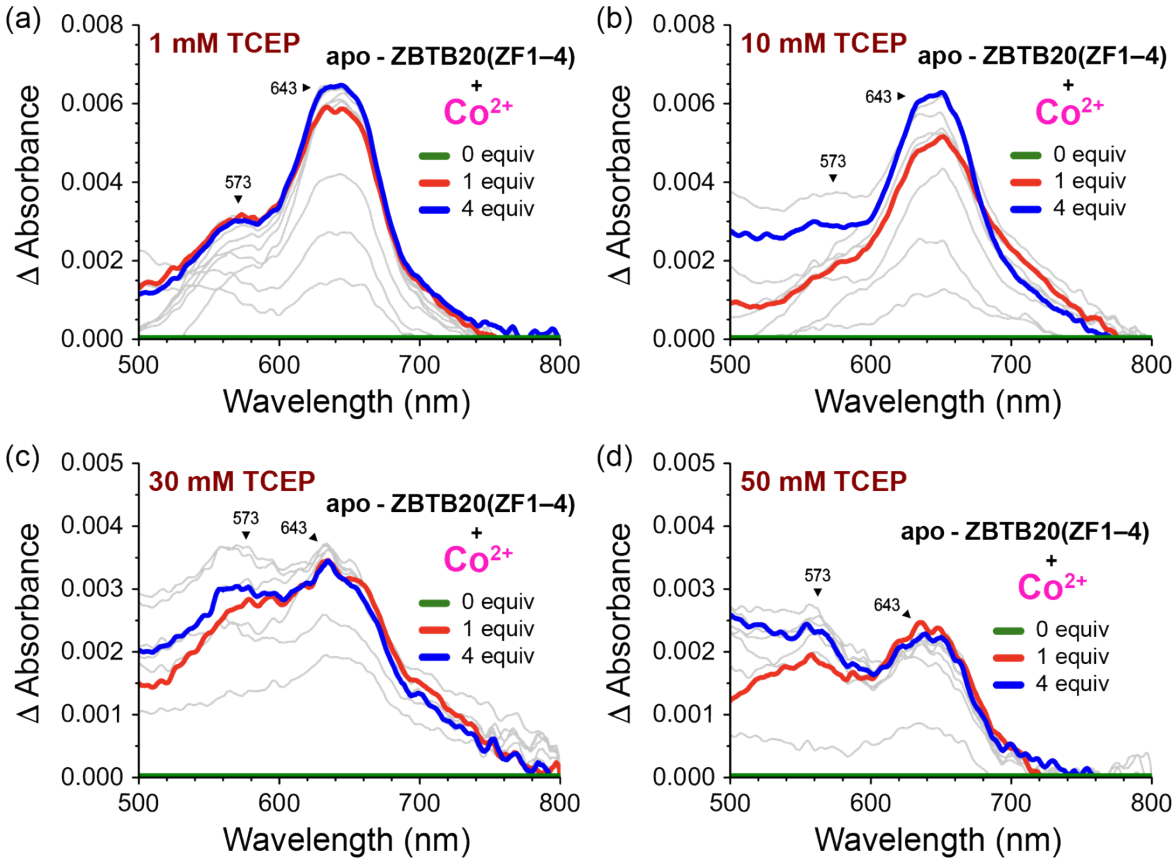

Figure S9. TCEP concentration-dependent oxidation of apo-ZBTB20(ZF1–4). Co^{2+}-induced d–d transition bands between 500 and 800 nm were monitored by UV–Visible spectroscopy, and were observed at 573 nm and 643 nm. Δ Absorbance represents the changes in absorbance relative to apo-ZBTB20(ZF1–4) upon Co^{2+} titration. Experiments were conducted in a buffer composed of 100 mM MOPS (pH 7.0) and 150 mM NaCl, with (a) 1 mM TCEP, (b) 10 mM TCEP, (c) 30 mM TCEP, or (d) 50 mM TCEP. Each experiment was performed inside an N_2(g)-filled glovebox.

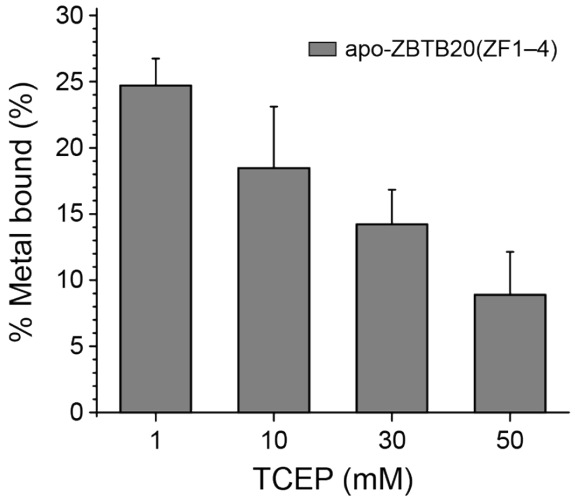

Figure S10. Comparison of % Metal bound under different TCEP concentrations. The metal binding percentage of apo-ZBTB20(ZF1–4) was determined using the absorbance maximum at 643 nm, corresponding to the Co^{2+}-dependent d–d transition band observed upon metal coordination, and assessed under varying TCEP concentrations. Error bars represent the standard deviation from five measurements.

Figure S11. Upstream sequence of the *brn2* promoter region from *Homo sapiens* (NCBI: NC_060930.1).[5]

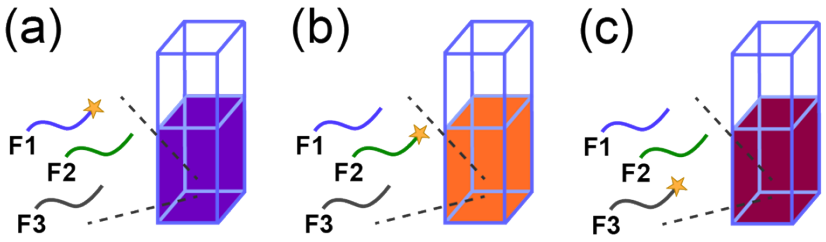

Figure S12. Schematic overview of the competition assay. (a–c) Competition assay using (a) 6-FAM labeled F1, (b) 6-FAM labeled F2, and (c) 6-FAM labeled F3. For each experiment, one fluorescently labeled *brn2* fraction and two unlabeled double-stranded *brn2* fractions were mixed in a buffer, with each DNA fraction diluted to 5 nM to maintain a 1:1:1 ratio. ZBTB20(ZF1–4) was titrated into the mixture at the indicated concentrations, followed by a 2-min incubation before measurement.

Protein	pH	TCEP (mM)	% Metal bound
ZBTB20(ZF1–4)	3.0	1.0	1.6 (± 1.1)
ZBTB20(ZF1–4)	4.0	1.0	1.4 (± 1.3)
ZBTB20(ZF1–4)	5.0	1.0	2.9 (± 2.0)
ZBTB20(ZF1–4)	6.0	1.0	24.8 (± 2.4)
ZBTB20(ZF1–4)	7.0	1.0	24.7 (± 2.0)
ZBTB20(ZF1–4)	7.4	1.0	19.6 (± 3.1)
ZBTB20(ZF1–4)	8.0	1.0	19.0 (± 5.2)
ZBTB20(ZF1–4)	7.0	10.0	18.5 (± 4.6)
ZBTB20(ZF1–4)	7.0	30.0	14.2 (± 2.6)
ZBTB20(ZF1–4)	7.0	50.0	8.9 (± 3.2)
ZBTB20(ZF1–5)	7.4	1.0	49.3 (± 5.4)

Table S1. % Metal bound of apo-ZBTB20(ZFs) under different pH and TCEP conditions.

Reference

1. H. Kim, Y. Hwang, J. S. Cheong and S. J. Lee, *RSC Chem. Biol.*, 2025, **6**, 1165-1173.
2. L. Yang, H. Xie, X. Wan, M. Li, M. Lv, Y. Duan, Y. Shi, W. J. Zhang and F. Li, *Structure*, 2025, **33**, 1398-1407.
3. K. Kluska, J. Adamczyk and A. Krężel, *Metallomics*, 2018, **10**, 248-263.
4. S. Park, Y. Hwang, K. S. Eom, J. S. Cheong and S. J. Lee, *Protein Sci.*, 2025, **34**, e70278.
5. M. Nagao, T. Ogata, Y. Sawada and Y. Gotoh, *Nat. Commun.*, 2016, **7**, 11102-11115.